Macromolecules

Article

pubs.acs.org/Macromolecules

Terms of Use

Lamellar Microdomains of Block-Copolymer-Based Ionic Supramolecules Exhibiting a Hierarchical Self-Assembly

Mehran Asad Ayoubi,*[,†] Kristoffer Almdal,[‡] Kaizheng Zhu,[§] Bo Nyström,[§] Ulf Olsson,[†] and Lennart Piculell[†]

[†]Division of Physical Chemistry, Center for Chemistry and Chemical Engineering, Lund University, SE-22 100 Lund, Sweden

[‡]Department of Micro- and Nanotechnology, Technical University of Denmark, DTU Nanotech, Building 423, DK-2800 Kongens Lyngby, Denmark

[§]Department of Chemistry, University of Oslo, P.O. Box 1033, Blindern N-0315 Oslo, Norway

Supporting Information

ABSTRACT: Based on a parent diblock copolymer of poly(styrene)-*b*-poly(methacrylic acid), PS-*b*-PMAA, linear-*b*-amphiphilic comb (L-*b*-AC) ionic supramolecules [*Soft Matter* **2013**, *9*, 1540−1555] are synthesized in which the poly(methacrylate) backbone of the ionic supramolecular AC-block is neutralized by alkyl (C*n*; *n* = 8, 12, and 16) trimethylammonium counterions (i.e., side chains) at various ion (pair) fractions *X* [i.e., counterion/side-chain grafting density; *X* = number of alkyl counterions (i.e., side chains) per acidic group of the parent PMAA block]—these L-*b*-AC ionic supramolecules exhibit a spherical-*in*-lamellar hierarchical self-assembly. For these systems, (1) the effective Flory−Huggins interaction parameter between L- and AC-blocks $\chi'_{Cn/X}$ was extracted, and (2) analysis of the lamellar microdomains showed that when there is an increase in *X*, alkyl counterion (i.e., side chain) length l_{sc}, or both, there is an increase in *both* the average interfacial area per block junction Σ and the thickness of the microlayer of the AC-block d_{AC}.

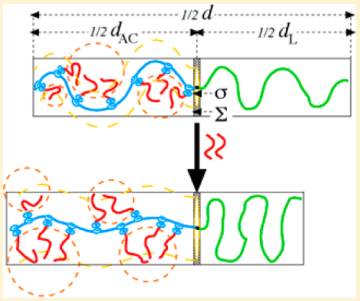

1. INTRODUCTION

Self-assembly of block copolymer-based systems has attracted a lot of attention due its fundamental importance and various useful applications.[1−3] For the melt of an A-*b*-B linear diblock copolymer, the interfacial tension between A- and B-blocks can drive the system into a microsegregated state in which segregated A-rich and B-rich microdomains exist. For such a system, it is now well established that, for a specific choice of A- and B-monomers, the shape of the well-segregated microdomains, being typically spherical (SPH), cylindrical (CYL), or lamellar (LAM), only depends on the volume ratio of the two blocks.[4,5]

By utilizing principles of supramolecular chemistry, it is possible to selectively attach amphiphile molecules to one of the blocks of an A-*b*-B diblock copolymer through physical bonds, e.g., via hydrogen[6−9] or ionic[10,11] bonds, and produce a block-copolymer-based supramolecule consisting of a linear block (A-block) and a comblike block (made up of a parent B-block and amphiphile molecules), i.e., a linear-*b*-comblike supramolecule. In such a system micro- and nanosegregation can occur simultaneously, giving rise to a variety of hierarchical structure-*in*-structure morphologies. Interestingly, while for both hydrogen-bonded and ionic-bonded based systems the shapes of the microdomains are typical of neat block copolymer systems (e.g., SPH, CYL, and LAM), those of the nanodomains may differ markedly, being LAM for hydrogen-bonded supramolecules[6−9,12−15] and SPH and CYL for ionic-bonded ones.[11]

Recently, possible nanotechnological applications of block copolymer−amphiphile supramolecules have attracted a lot of attention.[16−20] Obviously, for any nanotechnological application that utilizes self-assembly properties of such materials one of the essential first steps is establishment of the relationship(s) between the molecular (e.g., chemical and structural) and the self-assembly (e.g., shape and size of microdomains) properties of the system. Also, from a fundamental point of view, experimental determination of the major factors that define the relationship(s) between the molecular and self-assembly properties of such systems is important because it paves the way for development of theoretical models that correctly describe the experimental reality. Furthermore, it would be interesting to see if concepts and theories developed for conventional A-*b*-B diblock copolymers can be useful in simple rationalization of the self-assembly behavior of such complex systems. If this is the case, utilization of such concepts and theories can greatly facilitate design of experiments aiming to address specific fundamental questions or develop practical applications.

In ref 11 we presented results for a new class of block copolymer-based ionic supramolecules, composed of one linear block (L-block) and one *strongly* amphiphilic comblike block (AC-block), i.e., L-*b*-AC ionic supramolecule (see Figure 1),

Received: January 30, 2014
Revised: April 4, 2014
Published: May 13, 2014

 © 2014 American Chemical Society dx.doi.org/10.1021/ma500232y | *Macromolecules* 2014, 47, 3428−3435

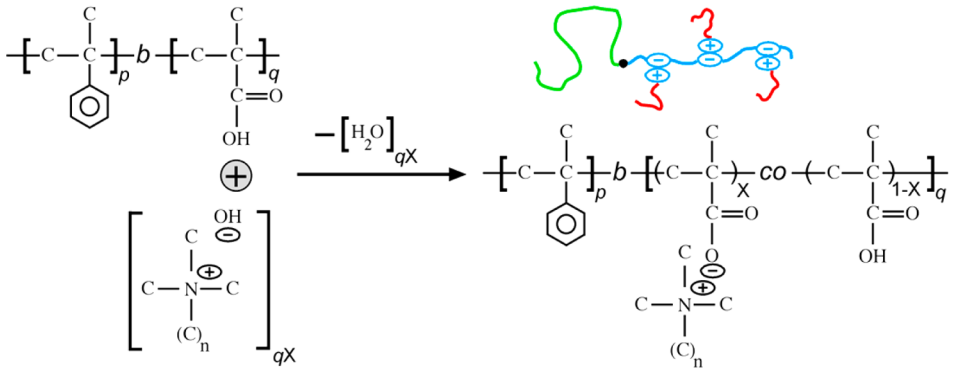

Figure 1. Schematic representations of the acid–base reaction between PMAA block of the PS-*b*-PMAA diblock copolymer and alkyltrimethylammonium hydroxide and the molecular architecture of the resultant linear-*b*-amphcomb (L-*b*-AC) ionic supramolecule.

exhibiting a two-scale structure-*in*-structure hierarchical self-assembly, where microsegregation (between L- and AC-blocks) and nanosegregation (between the polar P ionic backbone and the nonpolar NP alkyl side chains of the AC-block) occur simultaneously. These L-*b*-AC ionic supramolecules were synthesized via a selective acid–base reaction between hydroxide forms of alkyltrimethylammonium amphiphiles, C*n*TAOH, and acidic groups of poly(methacrylic acid), PMAA, blocks of diblock copolymers of poly(styrene)-*b*-poly(methacrylic acid), PS-*b*-PMAA. In this supramolecular synthesis procedure water molecules are eliminated, resulting in a diblock copolymer with one ionic supramolecular block (AC-block) composed of a poly(methacrylate) backbone neutralized by alkyltrimethylammonium counterions (see Figure 1). A key result of this study was that the *shape* of the microdomains is *only* dependent on the volume fraction of the AC-block Φ_{AC} *regardless* of the composition and the molecular weight of the parent diblock copolymer or of alkyl side chain (i.e., counterion) grafting density X [i.e., ion (pair) fraction; X = number of alkyl side chains (i.e., counterions) per acidic group of the parent PMAA block] and length l_{sc}. Thus, having established the relationship between the molecular properties of L-*b*-AC ionic supramolecules and the *shape* of the microdomains, the main aim of the present paper is to explore in detail the relationship between such properties and the *size* characteristics of the LAM microdomains of newly synthesized SPH-*in*-LAM exhibiting systems that are based on a not previously used diblock copolymer of PS-*b*-PMAA (S-MAA-M-17; see Table 1 for its molecular and structural characteristics) and C8, C12, and C16 counterions (i.e., side chains) at various X-values (X = 0.7, 0.8, 0.9, and 1.0) [such systems are symbolized as S-MAA-17-M/C*n*/X], using concepts developed for conventional A-*b*-B diblock copolymer systems.

2. EXPERIMENTAL DETAILS

Our block-copolymer-based ionic supramolecules are prepared by an acid–base reaction between the acidic groups of the PMAA block of S-MAA-17-M (see Table 1 for its molecular and structural characteristics) and the hydroxide forms of various alkyltrimethylamonium surfactants (C*n*TAOH, n = 8, 12, and 16) at varying X-values. In this process water is eliminated, and the alkyl counterions (i.e., side chains) [C8, C12, and C16] are tightly attached to the PMAA backbone through the trimethylammonium carboxylate ion pairs (please see Figure 1).

2.1. Materials. S-MAA-17-M was synthesized through the method of atom transfer radical polymerization (ATRP). Details of synthesis and characterization can be found in ref 21.

Table 1. Molecular and Structural Characteristic of the Parent Diblock Copolymers of L-*b*-AC Ionic Supramolecules for Which the Data Are Either Presented for the First Time or Are Reproduced from Ref 11

diblock copolymer	Z_{PS} [b]	Z_{PMAA} [b]	Φ_{PMAA} [c]	microdomain morphology [d]	
S-MAA-17-M[a]	155	43	0.17	SPH_{BCC} [e]	present paper[g]
S-MAA-15	318	78	0.15	SPH_{BCC} [e]	ref 11[h]
S-MAA-8-M[a]	155	18	0.08	SPH_{LL} [f]	ref 11[h]
S-MAA-3	440	17	0.03	SPH_{LL} [f]	ref 11[h]

[a]The diblock copolymer system contains a minor fraction of architecturally symmetric triblock molecules that are composed of PS end-blocks and PMAA mid-blocks. In the ATRP synthesis, these triblock molecules are the product of a coupling reaction between two diblock macroradicals.[21] [b]Z_i stands for the number-average degree of polymerization of an i-block. [c]Volume fraction of PMAA blocks Φ_{PMAA} is calculated from the density values ρ_{PMAA} = 1.22 g/cm^3 [22] and ρ_{PS} = 1.05 g/cm^3.[23] [d]Determined by SAXS analysis (the SAXS experiments were performed at the room temperature).[21] [e]SPH_{BCC} stands for spherical microdomains in body-centered-cubic arrangement. [f]SPH_{LL} stands for spherical microdomains in liquid-like state. [g]The related L-*b*-AC ionic supramolecules are synthesized for the present study, and the corresponding SAXS and size characteristics data are presented for the first time in the present paper. [h]The related L-*b*-AC ionic supramolecules were synthesized previously in ref 11, where all the SAXS data and a part of the size characteristics data can be found (the size characteristics data of L-*b*-AC ionic supramolecules needed for the analysis of the present paper are reproduced in Tables SI-1 and SI-2 of the Supporting Information).

The surfactants octyltrimethylammonium chloride (C8TACl), dodecyltrimethylammonium bromide (C12TABr), and hexadecyltrimethylammonium bromide (C16TABr) were purchased from TCI Europe. The corresponding hydroxide forms (C8TAOH, C12TAOH, and C16TAOH) were prepared using DOWEX MONOSPHERE 550 A (OH) anion exchange resin obtained from Sigma-Aldrich.

2.2. Sample Preparation. The surfactants were converted to their hydroxide forms (C*n*TAOH) by an ion-exchange reaction as described before,[24] and the dried C*n*TAOH powders were obtained after freeze-drying for several days.[11] Our samples of L-*b*-AC ionic supramolecules were prepared by adding desired small aliquots of C*n*TAOH as concentrated water/THF solutions to appropriate amounts of dioxane solutions of S-MAA-17-M followed by solvent evaporation and annealing steps, as was described in detail elsewhere.[11]

2.3. SAXS Measurements. SAXS measurements were performed at beamline I911-4 at the MaxLab synchrotron facility in Lund, Sweden. The intensity $I(q)$ was measured at room temperature as a function of the scattering vector q [$q = (4\pi/\lambda) \sin\theta$, where 2θ is the

dx.doi.org/10.1021/ma500232y | *Macromolecules* 2014, 47, 3428–3435

scattering angle and the wavelength of the X-ray beam was λ = 0.91 (Å)].

3. RESULTS AND STRUCTURAL/MOLECULAR ANALYSIS

In this section, for systems of L-*b*-AC ionic supramolecule, (i) SAXS results are provided (in subsection 3.1), (ii) SAXS-based structural analysis of the microsegregated state are presented (in subsection 3.2), (iii) the analogies with the conventional A-*b*-B diblock copolymer systems are elucidated (in subsection 3.3), (iv) nanosegregation related chain stretching of AC-blocks is discussed (in subsection 3.4), and (v) the existence of correlations between a molecular-packing characteristics of the AC-block and micro- and nanosegregation characteristics of the system is examined (in subsection 3.5).

3.1. SAXS Data. SAXS results are presented for L-*b*-AC ionic supramolecules of S-MAA-17-M/C*n*/*X* (*X* = 0.7, 0.8, 0.9, and 1.0) that are based on C8 (Figure 2a,b), C12 (Figure 2c,d), and C16 (Figure 2e,f) side chains.

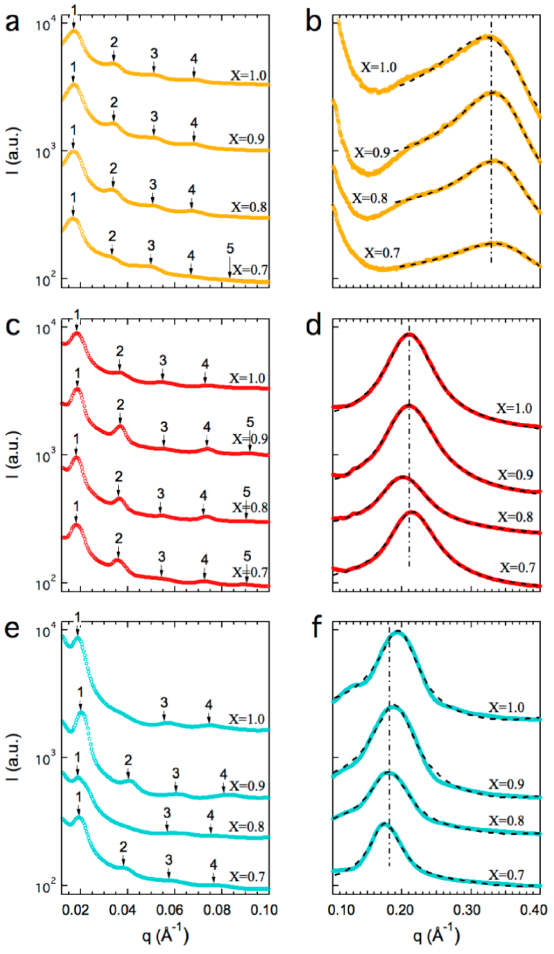

Figure 2. SAXS patterns of systems of S-MAA-17-M/C*n*/*X* (*X* = 0.7, 0.8, 0.9, and 1.0) for C8 (yellow) (a and b), C12 (red) (c and d), and C16 (e and f), at the low *q*-range (a, c, and e) and in the intermediate *q*-range (b, d, and e) are presented. In (a, c, and e) the observed reflections of LAM structure of the microdomains are indicated. In (b, d, and f) the dashed lines are the simulated intensities of the proposed model for the SPH nanodomains (eqs SI-1, SI-2, and SI-3 of the Supporting Information), and the dashed-dotted lines are the approximate positions of the broad peak. All the samples are birefringent when viewed between crossed-polarizers.

Examination of the scattering patterns in the low *q*-range (Figure 2a,c,e) and at the intermediate *q*-range (Figure 2b,d,f) is indicative of two behaviors. In the low *q*-range ($q \sim 0.01-0.1$ Å^{-1}), there are well-resolved reflections at integer relative positions. At the intermediate *q*-range ($q \sim 0.1-0.4$ Å^{-1}), a broad peak is present, with a position almost independent of the side-chain grafting density and centered at ca. 0.33, 0.21, and 0.18 Å^{-1} for C8, C12, and C16 containing L-*b*-AC ionic supramolecules, respectively. The reflections in the low *q*-range are attributed to a LAM structure and indicate that the system is microsegregated into alternating microlayers of L- and AC-blocks.[11] The broad peak at the intermediate *q*-range is related to the nanosegregated state of the AC-block, in which, due to the highly unfavorable P/NP interactions, NP alkyl side chains of the AC-block are segregated into spherical SPH nanodomains that are wrapped and separated by the P ionic backbone of the AC-block.[11] Thus, through simultaneous occurrence of micro- and nanosegregation, our L-*b*-AC ionic supramolecules exhibit a hierarchical SPH-*in*-LAM self-assembly.[11] (For characterization of the nanosegregated state please see the Supporting Information.)

3.2. Structural Analysis of Microdomains. Our L-*b*-AC ionic supramolecules, differing in their molecular characteristics through X and l_{sc}, are microsegregated into LAM microdomain morphology consisting of alternating microlayers of L- and AC-blocks. The values of the repeat distance of LAM microdomains *d* are presented in Table 2.

Table 2. Molecular and Microdomain Structural Characteristics of L-*b*-AC Ionic Supramolecules of S-MAA-17-M/C*n*/*X* Exhibiting LAM Microdomain Morphology As Revealed by SAXS Experiment Carried Out at Room Temperature

C*n*/*X*	Φ_{AC} [a]	*N* [b]	$q_{100} \times 10^5$ [c,d] (Å^{-1})	*d* [e] (Å)
C8/0.7	0.36	399	1657	379
C8/0.8	0.38	413	1683	373
C8/0.9	0.40	426	1694	371
C8/1.0	0.42	439	1700	370
C12/0.7	0.40	427	1809	347
C12/0.8	0.42	447	1798	349
C12/0.9	0.45	462	1837	342
C12/1.0	0.47	479	1817	346
C16/0.7	0.44	455	1905	330
C16/0.8	0.46	477	1872	336
C16/0.9	0.49	498	2028	310
C16/1.0	0.51	519	1855	339

[a]Volume fraction of the AC-block Φ_{AC} is calculated from the expression $\Phi_{AC} = \{[(1-X)v_{PMAA} + Xv_{PMAA-Cn}]Z_{PMAA}\}\{v_{PS}Z_{PS} + [(1-X)v_{PMAA} + Xv_{PMAA-Cn}]Z_{PMAA}\}^{-1}$, where v_i symbolizes the volume of the repeat unit of the *i*-species (PMAA-C*n* symbolizes the repeat unit of poly(alkylammonium methacrylate) with *n* carbon per alkyl side chain). We have v_{PS} = 165 Å^3 (from the density ρ value of ρ_{PS} = 1.05 g/cm^3), v_{PMAA} = 117 Å^3 (from ρ_{PMAA} = 1.22 g/cm^3), $v_{PMAA-C8}$ = 427 Å^3, $v_{PMAA-C12}$ = 520 Å^3, and $v_{PMAA-C16}$ = 613 Å^3 (we have assumed[11] a value of 1 g/cm^3 for $\rho_{PMAA-Cn}$). [b]*N* stands for the total number of segments of the system calculated using a reference volume of v_0 = 100 Å^3. [c]The position of the first SAXS peak of LAM structure q_{100} is determined by fitting a Gaussian to it. [d]The upper limits of uncertainty in the reported values of q_{100} are $\pm 5 \times 10^{-5}$ Å^{-1}. [e]The repeat distance of LAM structure *d* is calculated from $d = 2\pi/q_{100}$; the uncertainty in *d* is ±1 Å.

dx.doi.org/10.1021/ma500232y | Macromolecules 2014, 47, 3428−3435

An AC-block is ionic and dissolving it in the NP L-block (i.e., PS block) domains is energetically highly costly. Therefore, we assume that L- and AC-blocks are segregated into separate domains with no intermixing. (This assumption will be further substantiated in subsection 3.3.2; moreover, one needs to mention that it was experimentally shown that the parent S-MAA-17-M system exhibits strong-segregation-regime SSR behavior.[21]) Thus, from the known values of d, one is able to determine the thickness of the microlayer of the AC-block d_{AC} and the interfacial area per block junction Σ from the following expressions

$$d_{AC} = d\Phi_{AC} = dV_{AC}(V_L + V_{AC})^{-1} \quad (1)$$

$$\Sigma = 2d^{-1}(V_L + V_{AC}) \quad (2)$$

where the molecular volumes of the L-block (V_L) and the AC-block (V_{AC}) are calculated using values of (i) the side-chain grafting density (X), (ii) the segmental volumes (v_i), and (iii) the degrees of polymerization of the parent diblock copolymer system (Z_i) (see Tables 1 and 2 and their captions).

For various S-MAA-17-M/Cn/X systems the extracted values of d_{AC} and Σ are presented in Figure 3. It is observed that when X, l_{sc}, or both increase, there is an increase in *both* d_{AC} and Σ, in the ranges of 136 Å $\leq d_{AC} \leq$ 173 Å and 211 Å^2 $\leq \Sigma \leq$ 319 Å^2, respectively.

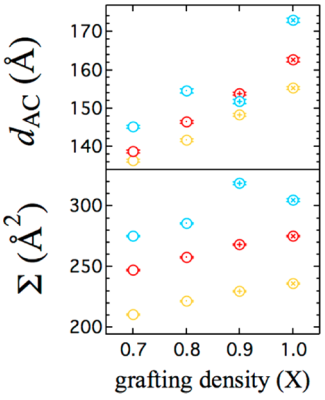

Figure 3. Variations of the thickness of the microlayer of the AC-block (d_{AC}) and the interfacial area per block junction (Σ) with the alkyl side-chain (i.e., counterion) grafting density (X) are shown for systems of S-MAA-17-M/Cn/X [X = 0.7 (hollow circle), 0.8 (circle with a dot), 0.9 (circle with a plus), and 1.0 (circle with a cross); C8 (yellow), C12 (red), and C16 (blue)].

3.3. Analogy with A-*b*-B Diblock Copolymer System.

In this subsection, in order to gain an insight over the microsegregation behavior of the system of L-*b*-AC ionic supramolecule, we establish analogies between its molecular and self-assembly characteristics and those of a system of A-*b*-B diblock copolymer, where, for simplicity, we ignore the possible effect(s) of the presence of the nanosegregated domains on the microsegregation behavior.

3.3.1. Effective Interaction Parameter. For an A-*b*-B diblock copolymer system, the self-consistent-field-theory (SCFT) of Helfand and Wasserman[25] (HW) predicts the following expression for the LAM domain spacing d

$$0 = -\frac{2\gamma}{k_B T}[Z_A v_A + Z_B v_B] + d + 0.353 \times \left[\frac{(Z_A{}^{0.5} v_A/b_A)^{2.5} + (Z_B{}^{0.5} v_B/b_B)^{2.5}}{(Z_A v_A + Z_B v_B)^{2.5}}\right] d^{3.5} \quad (3)$$

where γ = interfacial tension, k_B = Boltzmann constant, T = temperature, and b_i = statistical segment length of the i-block. Taking into account that (i) when Z_A, $Z_B \gg 1$, the second term can be ignored in comparison with the first and the third terms[26] and (ii) the interfacial tension and the Flory–Huggins interaction parameter are related by the following expression[27]

$$\frac{\gamma}{k_B T} = \frac{b_0}{v_0}\sqrt{\frac{\chi}{6}} \quad (4)$$

where v_0 is the reference segmental volume (throughout the present paper we have taken its value to be v_0 = 100 Å^3) and b_0 is the common statistical segment length (b_0 = geometric mean of the b values of the two blocks), after carrying out necessary notification changes and algebraic rearrangements, one obtains the following equation

$$d^7 = \frac{b_L b_{AC}}{6{v_0}^2}\left(\frac{2}{0.353}\right)^2 (V_L + V_{AC})^7 \times \left[\left(\frac{V_L}{Z_{PS}{}^{0.5} b_L}\right)^{2.5} + \left(\frac{V_{AC}}{Z_{PMAA}{}^{0.5} b_{AC}}\right)^{2.5}\right]^{-2} \chi'_{Cn/X} \quad (5)$$

where $\chi'_{Cn/X}$ is the effective Flory–Huggins interaction parameter between L- and AC-blocks, the latter bearing a particular counterion of Cn-type with an ion (pair) fraction of X.

For L-*b*-AC ionic supramolecule systems that differ in their parent diblock copolymer, but have the same Cn-type counterion (i.e., side chain) and ion (pair) fraction (X), one is able to determine $\chi'_{Cn/X}$ by linear regression, using (i) eq 5, (ii) (at least) two measured values of d (see Table 2 and Table SI-1 of the Supporting Information), and (iii) the values of the molecular parameters, including, among others, $b_L = b_{PS}$ = 6.8 Å[28] and for simplicity assumed value of $b_{AC} = b_{PMAA}$ = 6.2 Å [the value of 6.2 Å for b_{PMAA} is estimated from the radius of gyration of an unperturbed coil of PMAA;[21,29] also, please see ref 30]. The thus determined values of $\chi'_{Cn/X}$ are presented in Table 3 (for details of the regression analysis please see the Supporting Information).

3.3.2. Comparison with SSR and SCFT Theories. In our previous study[11] on L-*b*-AC ionic supramolecules based on diblock copolymers of PS-*b*-PMAA type and alkyl side chains (C8 and C12), in addition to LAM microdomains, liquidlike SPH microdomains and hexagonally packed CYL microdomains were also observed. For systems exhibiting SPH and CYL microdomain morphologies, it is useful to compare the experimental values for the radius of SPH microdomians R_{ex} and CYL microdomains R'_{ex} with those predicted by SSR and SCFT theories developed for A-*b*-B diblock copolymers, the latter obtained using values of $\chi'_{Cn/X}$ given in Table 3. Thus, the following theories were considered: SSR theories of Nyrkova et al.[31] (NKD) and Semenov et al.[32] (SNK) [for SPH microdomains] and the SCFT theory of Helfand and Wasserman[33] (HW) and the SSR theory of Semenov[34,35] (S) [for CYL microdomains]. The values of R_i (i = ex, NKD, and SNK) and R'_i (i = ex, HW, and S) are presented in Figure 4.

dx.doi.org/10.1021/ma500232y | Macromolecules 2014, 47, 3428–3435

Table 3. Room Temperature Effective Flory–Huggins Interaction Parameter for Systems Differing in Their C*n*-Type Counterion (i.e., Side-Chain) and Ion (Pair) Fraction (X)

C*n*	X	$\chi'_{Cn/X}$[a]
C8	0.8	1.1 ± 0.2
	1.0	1.9 ± 0.1
C12	0.8	0.8 ± 0.1
	1.0	0.5 ± 0.1
C16	0.9	1.8 ± 0.1
	1.0	3.0 ± 0.8

[a]Determined using eq 5 and d values of lamellae-forming L-*b*-AC ionic supramolecule systems (LAM microdomain morphology was identified by performing SAXS at the room temperature; the d values are listed in Table 2 and Table SI-1 of the Supporting Information). The standard deviation for each value of $\chi'_{Cn/X}$, obtained as a result of the linear regression procedure, is reported as the uncertainty interval (for details of the regression analysis please see Figure SI-2 of the Supporting Information).

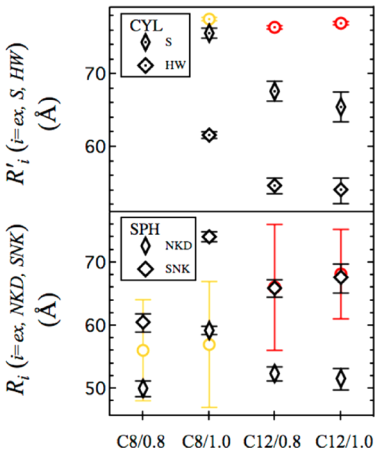

Figure 4. For L-*b*-AC ionic supramolecules that are based on parent diblock copolymers of (top) S-MAA-8-M (exhibiting CYL microdomain morphology) and (bottom) S-MAA-3 (exhibiting SPH microdomain morphology), the theoretical (black) and the experimental (yellow: C8-containing samples; red: C12-containing samples) radii of microdomains are shown (on the abscissa each system is designated by its side chain and X value, i.e., Cn/X) [experimental data are taken from ref 11 and are reproduced in Table SI-2 of the Supporting Information].

One can see that for both SPH and CYL microdomains the radii of microdomains predicted by the above-mentioned theories are usually either in excellent or close agreement with those experimentally obtained.

Before finishing this subsection, we point out that for LAM-forming L-*b*-AC ionic supramolecules for which the values of $\chi'_{Cn/X}$ are known, the average estimated thickness of the L/AC interface Δ is Δ = 3.3 ± 0.7 Å [using theory of Helfand[36,37]] and Δ = 3.7 ± 0.8 Å [using theory of Semenov[38]]. Thus, since $d/2 \gg \Delta$, the assumption made in subsection 3.2, stating that L- and AC-blocks are segregated into separate domains with no intermixing, is further justified.

3.3.3. Effective Degree of Segregation. For systems of L-*b*-AC ionic supramolecule, we have shown variation of d_{AC} with the effective microsegregation strength $\chi'_{Cn/X}N$ in Figure 5. It is observed that an increase in $\chi'_{Cn/X}N$ is accompanied by an increase in d_{AC}, suggesting that the higher the effective degree

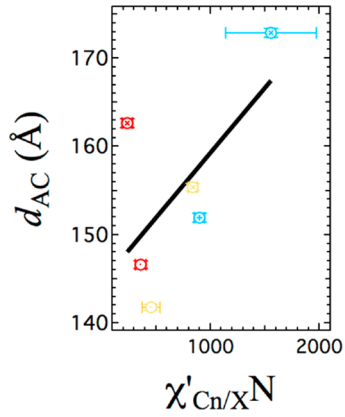

Figure 5. Variation of the thickness of the microlayer of the AC-block (d_{AC}) with the effective microsegregation strength ($\chi'_{Cn/X}N$) is shown. The black line is the result of fitting a line to the data and is meant to be guide for the eyes only. For information about the symbols and the colors please see caption of Figure 3.

of microsegregation $\chi'_{Cn/X}N$ the more stretched is the conformation of the backbone of the AC-block.

3.4. Nanosegregation within AC-Block. Within an AC-block nanosegregation occurs because the polar P ionic backbone and the nonpolar NP alkyl side chains tend to segregate. For facilitating the scientific reasoning, let us assume that hypothetical Flory–Huggins interaction parameters defined for each X value χ''_X (X = 0.7, 0.8, 0.9, and 1.0) can describe this thermodynamic incompatibility [one normally expect that $\chi''_{1.0} > \chi''_{1.9} > \chi''_{1.8} > \chi''_{1.7}$ because when the fraction of the ion pairs (X) increases, the backbone becomes more polar while the nonpolar chemical nature of the side chains remains unchanged]. Furthermore, for the AC-block, by taking a C–C backbone bond as the reference, we define the number of segments per C–C backbone bond N^* in the following manner (note that value of N^* for a system does not necessarily possess an integer value).

$$N^* = \frac{V_{AC}}{Z_{PMAA}} \times \frac{1}{v_0} \tag{6}$$

Thus, one can conveniently use the parameter $\chi''_X N^*$ as a measure of the effective degree of nanosegregation within the AC-block.

In Figure 6, values of the thickness of the microlayer of the AC-block d_{AC} for systems with different values of N^* are shown. It is observed that (i) for systems characterized by the same χ''_X (the data points connected by solid black lines) d_{AC} increases when N^* increases, (ii) for systems that have AC-blocks with the same l_{sc}, when there is an increase in X—and hence an increase in both N^* and χ''_X—there is an increase in d_{AC} (see the same-colored, dashed-line-connected data points), and (iii) the value of d_{AC} increases when—through an increase in both X and l_{sc}—both N^* and χ''_X increase. These observations suggest that an increase in the effective degree of nanosegregation $\chi''_X N$—caused by an increase in N^*, or both N^* and χ''_X [as explained above in (i)–(iii)]—is accompanied by an adoption of a more stretched conformation for the backbone of the AC-block.

3.5. Molecular-Packing Characteristics of AC-Block. For an AC-block, the side chains and the ion pairs constitute a large fraction of its total volume. Thus, an AC-block has a large

dx.doi.org/10.1021/ma500232y | Macromolecules 2014, 47, 3428–3435

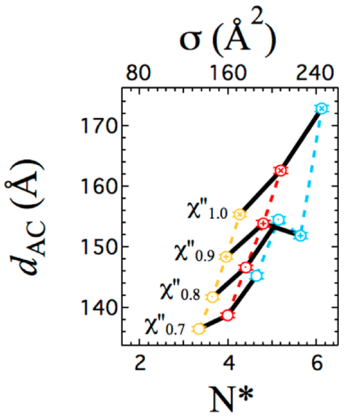

Figure 6. Variation of the thickness of the microlayer of the AC-block (d_{AC}) and the average molecular cross-sectional area (σ) with the number of segments per C−C bond of the AC-block (N^*) is shown. The data points connected by the solid black lines correspond to systems that are characterized b the same χ''_X. The data points connected by the colored dashed lines correspond to systems that are made up of the same type of counterion (i.e., side chain) but differ in their X values. For information about the symbols and the colors please see caption of Figure 3.

average molecular cross-sectional area σ defined in the following manner

$$\sigma = \frac{V_{AC}}{Z_{PMAA}} \times \frac{1}{\lambda_{con}} \tag{7}$$

where λ_{con} (= 2.5 Å) is the contour length of the repeat unit of the parent PMAA block.

From a purely volume-filling perspective, the lateral dimension of an AC-block dictates (i) its state of packing at the L/AC interface (quantitatively characterized by the value of Σ) and (ii) the degree of stretching of the backbone of the AC-block [depending on the extent of the crowding of the side chains and the ion pair atoms in the space close to the poly(methacrylate) part of the backbone]. Therefore, it would be useful to see how Σ and d_{AC} vary with σ. Regarding variation of Σ with σ, one can see that there is an increase in Σ when σ increases (see Figure 7). Regarding variation of d_{AC} with σ, one observes that, for systems having the same l_{sc} (in Figure 6, the same-colored, dashed-line-connected data points) or X (in Figure 6, the data points connected by the solid black lines), an increase in σ is accompanied by an increase in d_{AC}, suggesting that the higher the value of σ the more stretched is the conformation of the backbone of the AC-block.

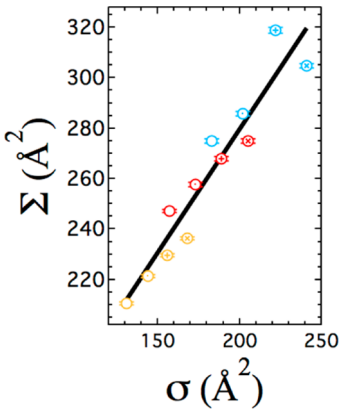

Figure 7. Variation of the average interfacial area per block junction (Σ) with the average molecular cross-sectional area of the AC-block (σ) is shown. The black line is the result of fitting a line to the data and is meant to be guide for the eyes only. For information about the symbols and the colors please see caption of Figure 3.

4. DISCUSSION

The L-*b*-AC ionic supramolecules studied in the present paper, being based on a parent diblock copolymer system of PS-*b*-PMAA (S-MAA-17-M; see Table 1) and alkyl side chains (i.e., counterions) of the C8, C12, and C16 type with various side-chain (i.e., counterion) grafting densities X (X = 0.7, 0.8, 0.9, and 1.0), exhibit SPH-*in*-LAM two-scale hierarchical self-assembly. In our previous study[11] on L-*b*-AC ionic supramoleucles based on other parent diblock copolymers of PS-*b*-PMAA (see Table 1), but the same side-chain (i.e., counterion) length l_{sc}, we showed that (i) the *shape* of the microdomains (being SPH, CYL, and LAM) is only dependent on the volume fraction of the AC-block Φ_{AC}, *regardless* of X and l_{sc}, and (ii) the LAM microdomain morphology was found in the Φ_{AC} range of $0.29 \leq \Phi_{AC} \leq 0.45$. The fact that, regardless of X and l_{sc}, the L-*b*-AC ionic supramolecules studied in the present paper show LAM microdomain morphology in the Φ_{AC} range of $0.36 \leq \Phi_{AC} \leq 0.51$ (see Table 2) is in line with what were stated above in (i) and (ii).

In block-copolymer-based systems, one method to determine the (effective) Flory−Huggins interaction parameter is based upon comparing the experimentally obtained microdomain size of well-segregated samples with the predictions of the available theories for the microdomain size.[35,39−44] Thus, using SCFT theory of HW[25] (eq 5), we have determined the effective Flory−Huggins interaction parameter between L- and AC-blocks $\chi'_{Cn/X}$ for systems containing counterion of Cn type and ion (pair) fraction of X (Table 3). The orders of magnitude of these $\chi'_{Cn/X}$ values are the same as the (effective) Flory−Huggins interaction parameters (χ) found in the literature[35,41−46] for a number of polymeric systems composed of P (ionic) and NP species. Also, it is observed that when X is increased, while $\chi'_{Cn/X}$ increases for C8- and C16-type counterions, it decreases for C12-type counterion (see Table 3). It is necessary to add that, for a number of polymeric systems composed of P ionic and NP species, literature reports pertaining to an increase[41−44] or a decrease[47,48] in χ upon an increase in the ion content of the system can be found. We also point out that the values of $\chi'_{Cn/X}$ acquired through using experimental data for LAM microdomains and SCFT theory of HW for A-*b*-B diblock copolymers are internally consistent because for other L-*b*-AC ionic supramolecules exhibiting SPH and CYL microdomain morphologies[11] (see Table SI-2 of the Supporting Information), a good agreement is observed between the experimentally obtained values of the radii of microdomains and those predicted by classical SSR and SCFT theories developed for A-*b*-B diblock copolymers (the latter obtained using $\chi'_{Cn/X}$ values listed in Table 3) [see Figure 4]. It should be added that, in line with issues highlighted in ref 44, the *d*-based method of extracting χ is particularly useful when determination of χ at order−disorder transition temperature T_{ODT}, or in the disordered state ($T > T_{ODT}$), is not feasible because the (anticipated) T_{ODT} is beyond the degradation temperature of the material. This is most likely applicable to our systems because it was shown in ref 21 that the used nonionic parent PS-*b*-PMAA block copolymers are in SSR. (This was inferred from the SAXS and the rheology

dx.doi.org/10.1021/ma500232y | *Macromolecules* 2014, 47, 3428−3435

experiments revealing that up to a temperature of ca. 230 °C the systems are microsegregated [block copolymer of S-MAA-17-M (used in the present article) and block copolymer of S-MAA-15 (used in our previous work[11])] or the estimated microsegregation strength [for block copolymer of S-MAA-18-M (used in our previous work[11])].) Nevertheless, while utilization of this method that provides an order-of-magnitude estimate of χ is useful for gaining an insight over the thermodynamics of the system under study, one should pay attention that in the process of determination of χ the uncertainties of the input parameters of the used theoretical model (e.g., the measured d-spacing; see eq 5) are largely amplified.[44]

In our L-*b*-AC ionic supramolecules we have observed that when X, l_{sc}, or both increase, *both* the average interfacial area per block junction Σ and the thickness of the microlayer of the AC-block d_{AC} increase (see Figures 3 and 8). Interestingly, we found that there is a clear correlation between Σ and the average molecular cross-sectional area of AC-block σ. More specifically, an increase in σ is accompanied by an increase in Σ (see Figure 7) [such a correlation is also observed for lamellae-forming L-*b*-AC ionic supramolecules of our previous study; see Figure SI-1 of Supporting Information]. Volume-filling considerations require that an increase in Σ must be accompanied by a decrease in the thickness of the microlayer of the L-block d_L, bringing about a more relaxed conformation for the L-blocks in the direction perpendicular to the L/AC interface (see Figure 8). Thus, thermodynamically, this increase in Σ is favorable because there is a gain in the conformational entropy of the L-blocks.

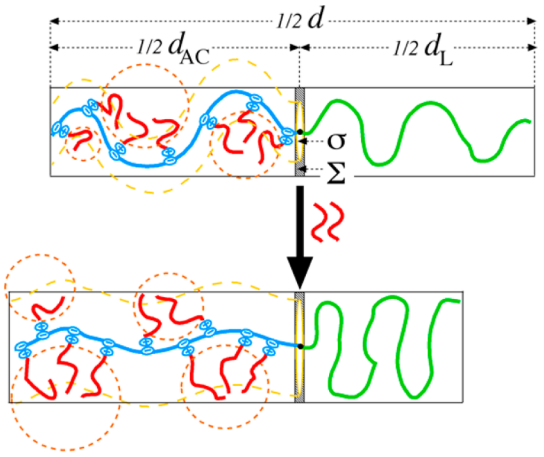

Figure 8. Schematics of the effects of increasing the side-chain (i.e., counterion) grafting density X on the molecular characteristics of the system, namely the average molecular cross-sectional area of AC-block σ, and the LAM microdomain characteristics of the system, including the thickness of the microlayer of the AC-block d_{AC}, the thickness of the microlayer of the L-block d_L, and the average interfacial area per block junction Σ [the same scenario holds valid when the side-chain (i.e., counterion) length l_{sc} or both X and l_{sc} are increased].

Regarding the increase in d_{AC}, we propose that it is mainly due to (i) the increased micro- and nanosegregation tendencies of the system, quantified by the parameters (*a*) effective degree of microsegregation between L- and AC-blocks ($\chi'_{Cn/X}N$) [see Figure 5] and (*b*) effective degree of nanosegregation between polar P and nonpolar NP components of the AC-block ($\chi''_X N^*$) [see Figure 6] and (ii) the crowding of the atoms of the side chains and the ion pairs in the space close to the poly(methacrylate) part of the backbone of the AC-block (see Figure 6). Thermodynamically, an increase in d_{AC} induces a loss in the conformational entropy of the backbone of the AC-block because it becomes more stretched (see Figure 8) but, apparently, (i) the favorable reduction in the total interfacial energy of the system [caused by less interfacial areas at L/AC and P/NP interfaces for the scenarios (*a*) and (*b*), respectively] and (ii) the fulfillment of the peculiar space-filling requirements of the atoms of the side chains and the ion pairs compensate for this entropic loss.

5. CONCLUSION

In this paper, L-*b*-AC ionic supramolecules based on a parent diblock copolymer of S-MAA-17-M and alkyl side-chains of the C8, C12, and C16 type with various side-chain grafting densities X (X = 0.7, 0.8, 0.9, and 1.0), exhibit SPH-*in*-LAM two-scale hierarchical self-assembly in an AC-block volume fraction window of $0.36 \leq \Phi_{AC} \leq 0.51$. The effective Flory–Huggins interaction parameter between L- and AC-blocks $\chi'_{Cn/X}$ was extracted for systems with various C*n*-type counterion (i.e., side chain) and ion (pair) fraction (X). Moreover, analysis of LAM microdomains of our L-*b*-AC ionic supramolecules showed that when there is an increase in X, side-chain length l_{sc}, or both, there is an increase in *both* the average interfacial area per block junction Σ and the thickness of the microlayer of the AC-block d_{AC}.

■ ASSOCIATED CONTENT

Supporting Information

Structural analysis of nanodomains; estimation of the statistical segment length of AC-block; tables showing molecular and structural characteristics of some of L-*b*-AC ionic supramolecules of ref 11 exhibiting LAM (Table SI-1), CYL and SPH (Table SI-2) microdomain morphologies; Figure SI-1 showing variation of Σ with σ for lamellae-forming S-MAA-15/C*n*/X and S-MAA-8-M/C*n*/X L-*b*-AC ionic supramolecules of ref 11; Figure SI-2 detailing the regression analysis regarding determination of $\chi'_{Cn/X}$. This material is available free of charge via the Internet at http://pubs.acs.org.

■ AUTHOR INFORMATION

Corresponding Author

*E-mail Mehran_Asad_Ayoubi@yahoo.com (M.A.A.).

Notes

The authors declare no competing financial interest.

■ ACKNOWLEDGMENTS

Financial support by the Swedish Research Council (VR) through the Linnaeus grant for the Organizing Molecular Matter (OMM) Center of Excellence (2009-6794) is gratefully acknowledged.

■ REFERENCES

(1) Hamley, I. *The Physics of Block Copolymers*; Oxford University Press: New York, 1998; 432 pp.
(2) Hamley, I. W. *Angew. Chem., Int. Ed.* **2003**, *42*, 1692–1712.
(3) Darling, S. B. *Prog. Polym. Sci.* **2007**, *32*, 1152–1204.
(4) Bates, F. S.; Fredrickson, G. H. *Annu. Rev. Phys. Chem.* **1990**, *41*, 525–557.
(5) Bates, F. S.; Schulz, M. F.; Khandpur, A. K.; Förster, S.; Rosedale, J. H.; Almdal, K.; Mortensen, K. *Faraday Discuss.* **1994**, *98*, 7–18.

(6) Ruokolainen, J.; Mäkinen, R.; Torkkeli, M.; Mäkelä, T.; Serimaa, R.; Ten Brinke, G.; Ikkala, O. *Science* **1998**, *280*, 557−560.
(7) Ruokolainen, J.; Saariaho, M.; Ikkala, O.; Ten Brinke, G.; Thomas, E. L.; Torkkeli, M.; Serimaa, R. *Macromolecules* **1999**, *32*, 1152−1158.
(8) Ruokolainen, J.; Ten Brinke, G.; Ikkala, O. *Adv. Mater.* **1999**, *11*, 777−780.
(9) Valkama, S.; Ruotsalainen, T.; Nykänen, A.; Laiho, A.; Kosonen, H.; Ten Brinke, G.; Ikkala, O.; Ruokolainen, J. *Macromolecules* **2006**, *39*, 9327−9336.
(10) Thünemann, A. F.; General, S. *Macromolecules* **2001**, *34*, 6978−6984.
(11) Ayoubi, M. A.; Zhu, K.; Nyström, B.; Almdal, K.; Olsson, U.; Piculell, L. *Soft Matter* **2013**, *9*, 1540−1555.
(12) Tsao, C. S.; Chen, H. L. *Macromolecules* **2004**, *37*, 8984−8991.
(13) Nandan, B.; Lee, C. H.; Chen, H. L.; Chen, W. C. *Macromolecules* **2005**, *38*, 10117−10126.
(14) Nandan, B.; Lee, C. H.; Chen, H. L.; Chen, W. C. *Macromolecules* **2006**, *39*, 4460−4468.
(15) Sart, G. G. D.; Vukovic, I.; Van Ekenstein, G. A.; Polushkin, E.; Loos, K.; Brinke, G. T. *Macromolecules* **2010**, *43*, 2970−2980.
(16) Valkama, S.; Ruotsalainen, T.; Kosonen, H.; Ruokolainen, J.; Torkkeli, M.; Serimaa, R.; Ten Brinke, G.; Ikkala, O. *Macromolecules* **2003**, *36*, 3986−3991.
(17) Bondzic, S.; De Wit, J.; Polushkin, E.; Scheuten, A. J.; Brinke, G. T.; Ruokolainen, J.; Ikkala, O.; Dolbnya, I.; Bras, W. *Macromolecules* **2004**, *37*, 9517−9524.
(18) Ruotsalainen, T.; Turku, J.; Heikkilä, P.; Ruokolainen, J.; Nykänen, A.; Laitinen, T.; Torkkeli, M.; Serimaa, R.; Brinke, G. T.; Harlin, A.; Ikkala, O. *Adv. Mater.* **2005**, *17*, 1048−1052.
(19) Ruotsalainen, T.; Turku, J.; Hiekkataipale, P.; Vainio, U.; Serimaa, R.; Brinke, G. T.; Harlin, A.; Ruokolainen, J.; Ikkala, O. *Soft Matter* **2007**, *3*, 978−985.
(20) Nandan, B.; Kuila, B. K.; Stamm, M. *Eur. Polym. J.* **2011**, *47*, 584−599.
(21) Asad Ayoubi, M.; Zhu, K.; Nyström, B.; Olsson, U.; Almdal, K.; Khokhlov, A. R.; Piculell, L. *J. Polym. Sci., Part B: Polym. Phys.* **2013**, *51*, 1657−1671.
(22) Walter, H.; Harrats, C.; Müller-Buschbaum, P.; Jérome, R.; Stamm, M. *Langmuir* **1999**, *15*, 1260−1267.
(23) Mark, J.; Ngai, K.; Graessley, W.; Mandelkern, L.; Samulski, E.; Koenig, J.; Wignall, G. *Physical Properties of Polymers*, 3rd ed.; Cambridge University Press: Cambridge, 2004; 536 pp.
(24) Svensson, A.; Piculell, L.; Cabane, B.; Ilekti, P. *J. Phys. Chem. B* **2002**, *106*, 1013−1018.
(25) Helfand, E.; Wasserman, Z. R. *Macromolecules* **1976**, *9*, 879−888.
(26) Matsushita, Y.; Mori, K.; Saguchi, R.; Nakao, Y.; Noda, I.; Nagasawa, M. *Macromolecules* **1990**, *23*, 4313−4316.
(27) Helfand, E.; Sapse, A. M. *J. Chem. Phys.* **1975**, *62*, 1327−1331.
(28) Ballard, D. G. H.; Wignall, G. D.; Schelten, J. *Eur. Polym. J.* **1973**, *9*, 965−969.
(29) Pleštil, J.; Ostanevich, Y. M.; Bezzabotonov, V. Y.; Hlavatá, D.; Labský, J. *Polymer* **1986**, *27*, 839−842.
(30) Assuming a value of 6.2 Å for the statistical segment length of the AC-block of systems that have various side-chain length and grafting density is reasonable because it is very close to the estimated value of 6.3 Å obtained by utilizing the results of the SCFT theory (Matsen, M. W.; Bates, F. S. *J. Polym. Sci., Part B: Polym. Phys.* **1997**, *35*, 945−952) and the experimental microdomain morphological diagram of ref 11 (for details please see the Supporting Information). Also, the simplifying assumption that the statistical segment lengths of the AC-block of our systems are the same as the parent PMAA block is in line with the fact that the statistical segment lengths of poly(methyl methacrylate) (PMMA), poly(butyl methacrylate) (PBMA), and poly(pentyl methacrylate) (PPMA) [= 6.6, 7.3, and 7.1 Å, respectively; calculated from data of Eitouni, H. B.; Balsara, N. P. In *Physical Properties of Polymers Handbook*; Springer: New York, 2007; pp 339−356, when, instead of a constant value of 100 $Å^3$ (used in the handbook), the reference volume is the "chemical monomer" repeat unit] are fairly similar.
(31) Nyrkova, I. A.; Khokhlov, A. R.; Doi, M. *Macromolecules* **1993**, *26*, 3601−3610.
(32) Semenov, A. N.; Nyrkova, I. A.; Khokhlov, A. R. *Macromolecules* **1995**, *28*, 7491−7500.
(33) Helfand, E.; Wasserman, Z. R. *Macromolecules* **1980**, *13*, 994−998.
(34) Semenov, A. N. *Sov. Phys.—JETP* **1985**, *61*, 733−742.
(35) Clarke, C. J.; Eisenberg, A.; La Scala, J.; Rafailovich, M. H.; Sokolov, J.; Li, Z.; Qu, S.; Nguyen, D.; Schwarz, S. A.; Strzhemechny, Y.; Sauer, B. B. *Macromolecules* **1997**, *30*, 4184−4188.
(36) Helfand, E.; Tagami, Y. *J. Polym. Sci., Part B: Polym. Lett.* **1971**, *9*, 741−746.
(37) Helfand, E.; Tagami, Y. *J. Chem. Phys.* **1972**, *56*, 3592−3601.
(38) Semenov, A. N. *Macromolecules* **1993**, *26*, 6617−6621.
(39) Ren, Y.; Lodge, T. P.; Hillmyer, M. A. *Macromolecules* **2000**, *33*, 866−876.
(40) Davidock, D. A.; Hillmyer, M. A.; Lodge, T. P. *Macromolecules* **2003**, *36*, 4682−4685.
(41) Park, M. J.; Balsara, N. P. *Macromolecules* **2008**, *41*, 3678−3687.
(42) Young, W. S.; Epps, T. H. *Macromolecules* **2009**, *42*, 2672−2678.
(43) Young, W. S.; Albert, J. N. L.; Schantz, A. B.; Epps, T. H. *Macromolecules* **2011**, *44*, 8116−8123.
(44) Hernandez, N.; Benson, C.; Cochran, E. W. *Macromolecules* **2013**, *46*, 179−187.
(45) Tan, N. C. B.; Liu, X.; Briber, R. M.; Peiffer, D. G. *Polymer* **1995**, *36*, 1969−1973.
(46) Zhou, N. C.; Xu, C.; Burghardt, W. R.; Composto, R. J.; Winey, K. I. *Macromolecules* **2006**, *39*, 2373−2379.
(47) Teran, A. A.; Balsara, N. P. *J. Phys. Chem. B* **2014**, *118*, 4−17.
(48) Huang, J.; Tong, Z.-Z.; Zhou, B.; Xu, J.-T.; Fan, Z.-Q. *Polymer* **2013**, *54*, 3098−3106.